Spring 2023

Structural Engineering of Thermostable Fluorescent Proteins TGP-E and YTP-E and Crystal Structure of TGP-E

Matthew Ryan Anderson
Missouri State University, Anderson9872@live.missouristate.edu

STRUCTURAL ENGINEERING OF THERMOSTABLE FLUORESCENT PROTEINS TGP-E AND YTP-E AND CRYSTAL STRUCTURE OF TGP-E

A Master's Thesis

Presented to

The Graduate College of

Missouri State University

In Partial Fulfillment

Of the Requirements for the Degree

Master of Science, Chemistry

By

Matthew Anderson

May 2023

STRUCTURAL ENGINEERING OF THERMOSTABLE FLUORESCENT PROTEINS TGP-E AND YTP-E AND CRYSTAL STRUCTURE OF TGP-E

Chemistry

Missouri State University, May 2023

Master of Science

Matthew Anderson

ABSTRACT

Thermostable fluorescent proteins, such as thermal green protein (TGP) and yellow thermal protein (YTP), could be used as biosensors to monitor cellular activity and as a fusion tag to monitor a protein of interest. The use of fluorescent proteins can sometimes be limited in certain organelles with low pH and in thermophilic organisms. This research aims to improve the thermal stability of TGP and YTP. TGP was created from a synthetically derived eCGP123 protein to improve solubility by substituting residues on the positively charged β- barrel surface with negatively charged glutamate (E) at Los Alamos National Lab. YTP was developed by mutating a histidine residue located under the chromophore into a tyrosine (H193Y) by the DeVore lab. The properties in which we are targeting improvement are thermal stability, pH stability, overall fluorescence, and the ability to withstand extreme conditions. To accomplish this overall improvement, we altered the chromophore using sited-directed mutagenesis to mutate glutamine 66 to glutamate in both YTP and TGP proteins. The YTP-E protein improved the thermal stability and the overall pH stability compared to TGP-E and YTP. A TGP-E protein crystal structure was obtained with a resolution of 2 Å which gave us insight that there is an additional hydrogen bond formed between Glu 66 and the backbone. The conserved hydrogen bond became shorter than in TGP, making TGP-E more stable - which explains the changes to the protein's properties.

KEYWORDS: thermostable, fluorescent, protein, GFP, TGP, X-ray diffract, stability

STRUCTURAL ENGINEERING OF THERMOSTABLE FLUORESCENT PROTEINS TGP-E AND YTP-E AND CRYSTAL STRUCTURE OF TGP-E

By

Matthew Anderson

A Master's Thesis
Submitted to the Graduate College
Of Missouri State University
In Partial Fulfillment of the Requirements
For the Degree of Master of Science, Chemistry

May 2023

Approved:

Natasha DeVore, Ph.D., Thesis Committee Chair

Gautam Bhattacharyya, Ph.D., Committee Member

Tuhina Banerjee, Ph.D., Committee Member

Christopher Lupfer, Ph.D., Committee Member

Julie Masterson, Ph.D., Dean of the Graduate College

ACKNOWLEDGEMENTS

I would first like to thank Dr. DeVore for allowing me to be a part of her research lab over the past three years. During that time, she has shown so much patience in helping me further my understanding and research. I would also like to thank the chemistry and biology grad students for your support. I would like to give a special shout-out to Autumn, Collin, Giselle, Megan Westwood, Dylan, and Cora. They were all there when I needed someone to talk to, helped me push to finish, and I will remember all the good times we have shared. I would also like to say thanks to my mom for always supporting me and believing in me even when others had their doubts. This support system has helped me push through to get to where I am today.

I dedicate this thesis to my mom, Michelle Anderson, for always supporting me and being there.

TABLE OF CONTENTS

LIST OF TABLES

LIST OF FIGURES

INTRODUCTION

The discovery of the green fluorescent protein (GFP) by Shimomura et al.[1] and further development through cloning, expression,[2] and engineering for desirable colors and properties have caused fluorescent proteins (FPs) to become an indispensable tool for multiple areas of research.[3,4] The FPs are useful since the chromophore can form without enzymes or cofactors and only require molecular oxygen to form.[5] The properties of GFP can be altered by mutations of specific protein residues which can lead to changes in the excitation and emission or allow faster protein folding.[6,7] Mutations can also allow for the further development of other useful properties such as biosensors and photo-switching properties.[8,9]

These fluorescent proteins have many uses across many scientific fields such as fluorescent tagging/ labeling. This occurs when a fluorescent protein is fused to a biological system of interest, allowing intracellular molecular imaging.[10] The tagging allows for monitoring of gene activation, selective labeling, and analysis of single proteins, cellular organelles, and whole cells.[11] This process of tagging a protein of interest to fluorescent proteins allows for *in vivo* studies to occur and allows for visualization of the localization of these proteins in tissues, cells, or subcellular compartments.[11] For example, a cancer study from 2018 used fluorescent tagging with a cell line that is known to cause breast cancer. The researchers used mice as test subjects and injected the GFP-tagged cell line into the mammary glands of the mice (Figure 1). They were able to see where the tumors localized based on the fluorescent tags that were within the cell line.[12] This use of fluorescent tagging can give us insight into cellular activity, but it is not the only use for these fluorescent proteins.

In the past ten years, fluorescent biosensors have made great progress and are widely used in biology, medicine, chemistry, and other fields.[13] Fluorescent biosensors can be used as ultra-sensitive detection to many biomolecules such as nucleic acids, proteins, enzymes, ATP, metal ions, and pH.[13,14] For example, a research group created a fluorescent biosensor that is pH sensitive; as the pH lowers, gaining more hydrogen ions, the intensity of the protein fluorescence increases (Figure 2). Advancements such as the one seen in Figure 2 can allow for lower-cost tests that also reduce the need to bring instrumentation to the field. The fluorescent biosensors have many other advantages such as being easy to use, fast response time, multiple analyses, high sensitivity, and good selectivity.[13] These biosensors can greatly improve field work and medical tests while providing a fast and efficient result that does not require years of training like comparable instrumentation. Both biosensors and fluorescent tagging can help further development of research in multiple fields in the scientific community.

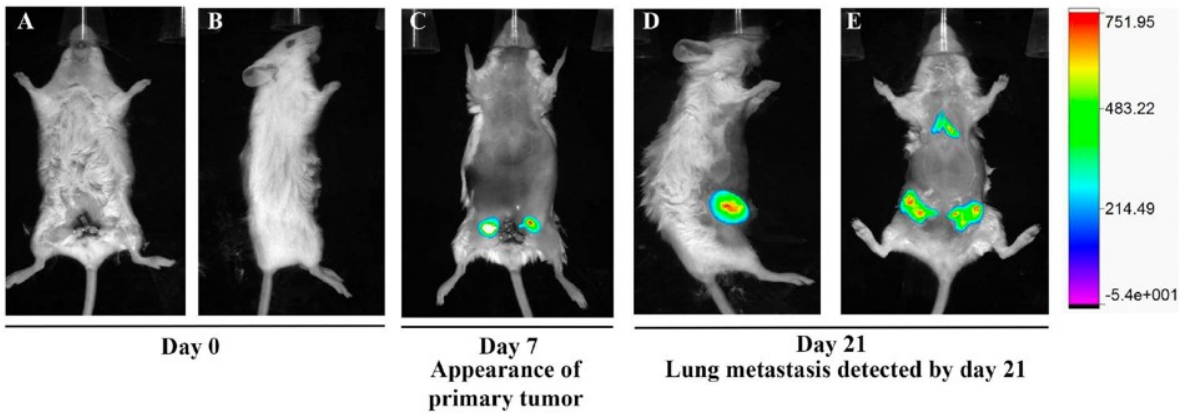

Figure 1. In vivo imaging of GFP-tagged tumor-bearing mice adapted from Ghosh et al.[12]

Fluorescence occurs as a two-step chemical reaction involving the absorption of light at a shorter-wavelength.[15] This light is then absorbed by a chemical fluorophore or chromophore of a protein which is called excitation.[15] An example of what a chromophore would look like for a

fluorescent protein (typically made of three protein residues) can be seen in Figure 3. Once the chromophore released energy, it causes a longer wavelength of light to be released known as the emission. This phenomenon can be visualized in Figure 4, displaying how the absorption of light starts from the ground state and then excites the electrons within the chromophore of the protein, increasing the energy level. Once released, the emission of the energy allows for visible fluorescence.

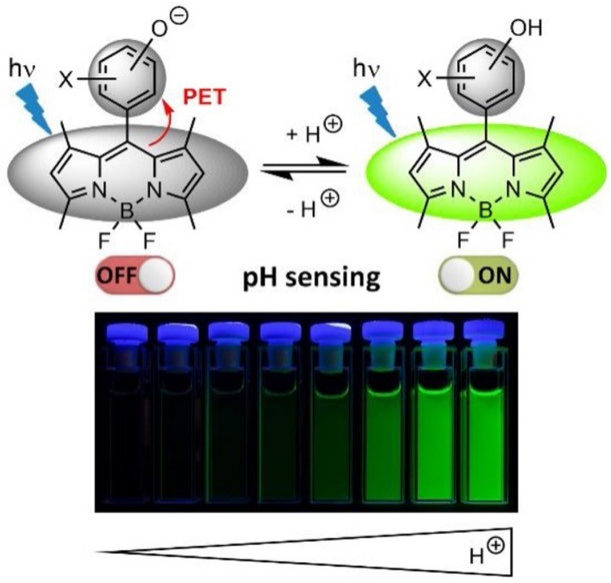

Figure 2. Example of a GFP biosensor that activates as the pH lowers adapted from Radunz et al.[14] CC BY 4.0, https://creativecommons.org/licenses/by/4.0/, no changes were made.

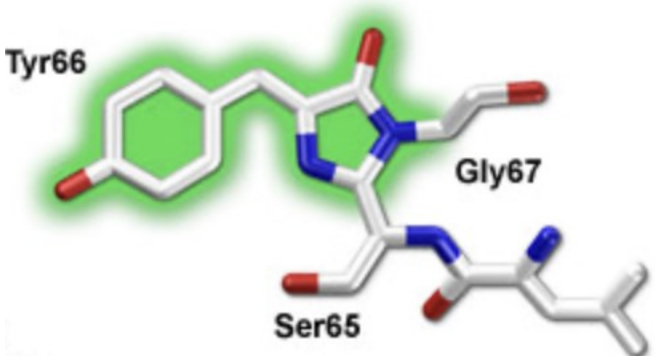

Figure 3. Chromophore of GFP adapted from Piston et al.[16]

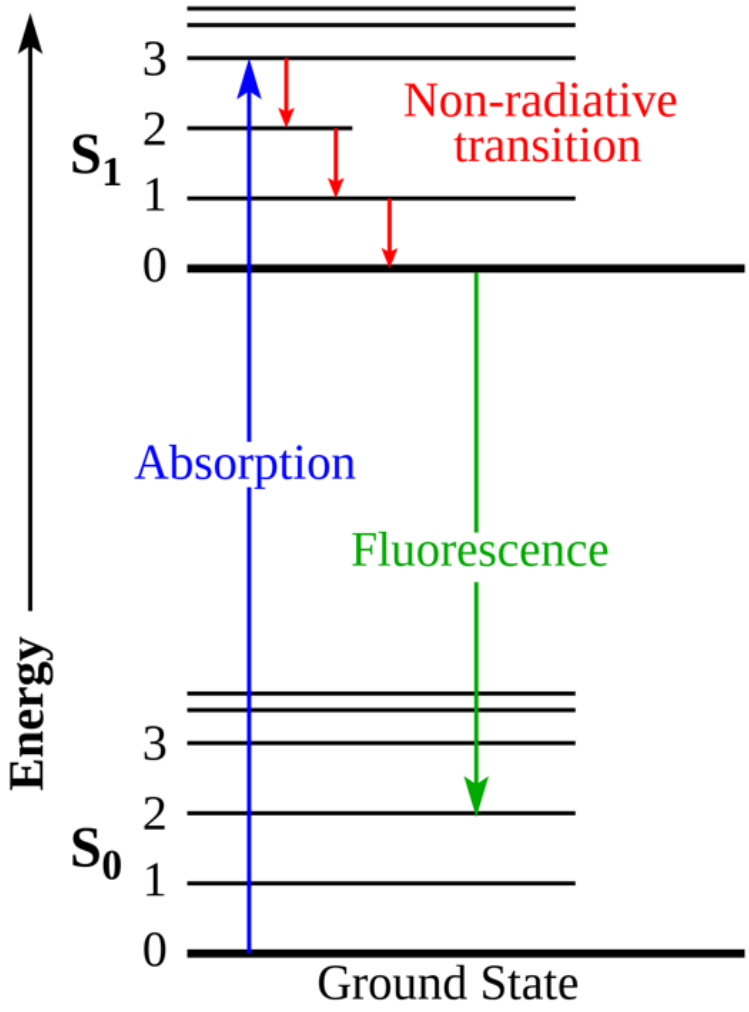

Figure 4. Jablonski diagram of absorbance and fluorescence adapted from Mooney et al.[17]

Now that there has been a background on fluorescent proteins and how they work, it is time to establish the starting point for the research that was completed. Thermal green protein (TGP) (RCSB PDB 4TZA) is the starting protein used in the research that will be discussed. TGP is an 11 stranded β-barrel protein which is an array of beta-strands arranged antiparallel to each other with a hydrogen bonding networking between nearby strands that are adjacent to the amino acid sequences.[18,19] Figure 5 shows the anti-parallel beta sheets that form a β- barrel in the structure of TGP. Like other fluorescent proteins, it contains a central α helix that contains

three residues (QYG) that form its chromophore. The central α helix is displayed in Figure 5 and the QYG chromophore of TGP can be seen in Figure 6. Due to the structure of β- barrel proteins, they are very stable. The stability of these proteins occurs from their extensive hydrogen bonding network making them an ideal protein for thermal stability, with many of their melting temperatures being around 80 °C.[20]

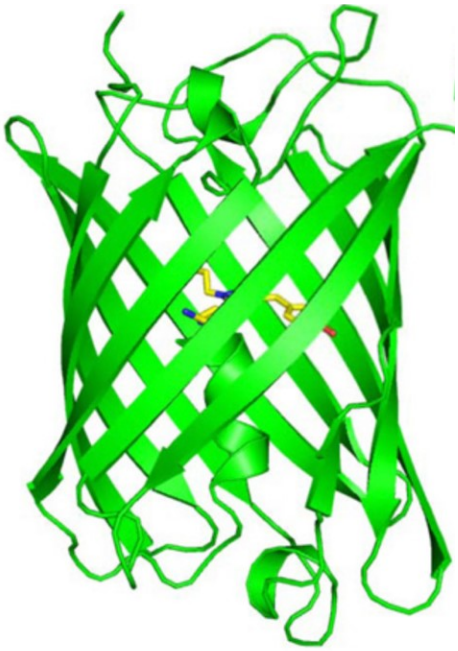

Figure 5. TGP beta-barrel structure adapted from Close et al.[19]

Despite TGP containing the β- barrel structure for stability, it is unusual compared to most fluorescent proteins. This is due to TGP being non-aggregation-prone and a highly soluble fluorescent protein.[21] TGP was engineered from eCGP123 (CGP consensus green protein). The eCGP123 protein was derived from the synthetic consensus green protein (CGP) with directed evolution to improve the thermostability.[21,22] The CGP protein has the closest identity at 85.5 % identical to the monomeric Azami-Green (mAG) protein which was isolated from stony coral *Galaxea fasciclairs*.[23] The mAG is the very first known monomeric green-emitting fluorescent

protein that was not derived from GFP.[23] TGP has only an 87% identity to monomeric green (mAG) from *Galaxea fascicularis* and 33.3% identity to the *Aequorea victorica* GFP.[24] While TGP has the same chromophore naturally found from mAG and also found in the red fluorescent protein DsRed (QYG) - previously discussed above and featured in Figure 6- GFP has an entirely different chromophore that is SYG - seen in Figure 3.[23,25,3] TGP is a synthetically derived protein which has a small identity and different chromophore than naturally occurring GFP, showing they are distinctly different proteins.

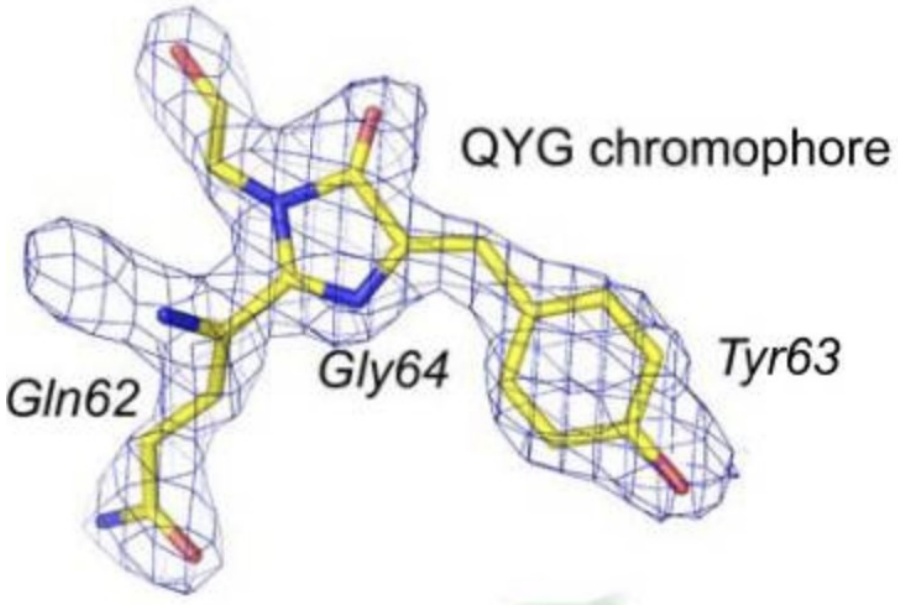

Figure 6. TGP QYG chromophore adapted from Close et al.[19]

Despite TGP containing the β- barrel structure for stability, it is unusual compared to most fluorescent proteins. This is due to TGP being non-aggregation-prone and a highly soluble fluorescent protein.[21] TGP was engineered from eCGP123 (CGP consensus green protein). The eCGP123 protein was derived from the synthetic consensus green protein (CGP) with directed evolution to improve the thermostability.[21,22] The CGP protein has the closest identity at 85.5 %

identical to the monomeric Azami-Green (mAG) protein which was isolated from stony coral *Galaxea fasciclairs*.[23] The mAG is the very first known monomeric green-emitting fluorescent protein that was not derived from GFP.[23] TGP has only an 87% identity to monomeric green (mAG) from *Galaxea fascicularis* and 33.3% identity to the *Aequorea victorica* GFP.[24] While TGP has the same chromophore naturally found from mAG and also found in the red fluorescent protein DsRed (QYG) - previously discussed above and featured in Figure 6- GFP has an entirely different chromophore that is SYG - seen in Figure 3.[23,25,3] TGP is a synthetically derived protein which has a small identity and different chromophore than naturally occurring GFP, showing they are distinctly different proteins.

There has been an influx of new development of GFP-like proteins to derive the most desirable qualities, allowing them to outperform GFP standards. For example, CGP was synthesized based on the consensus alignment of 31 different fluorescent protein amino acid sequences to gain the most desirable qualities in one protein.[26] Then using direct evolution of CGP leads to eCGP123 with improved thermostability that outperformed mAG. TGP was designed to improve solubility since many of the fluorescent proteins have issues with aggregation.[19] Improved solubility was achieved by substituting positively charged residues on the β-barrel surface with negatively charged glutamates (E).[19] This allows TGP to have strong advantages over other available FPs in experiments utilizing harsh thermophilic conditions or when protein aggregation affects assay results - for example in amyloid assays.[7,22,27] TGP has also been used to construct a chimera between light and heavy chain variable regions of antibodies, allowing a one-step fluorescent assay for fluorescent-activated cell sorting.[28] Figure 7 displays the diagram of TGP being fused between light and heavy chains of antibodies. TGP

tagging worked better than the standard GFP due to TGP being able to withstand more oxidizing environments. This indicates that TGP is more pH stable in acidic environments than GFP.

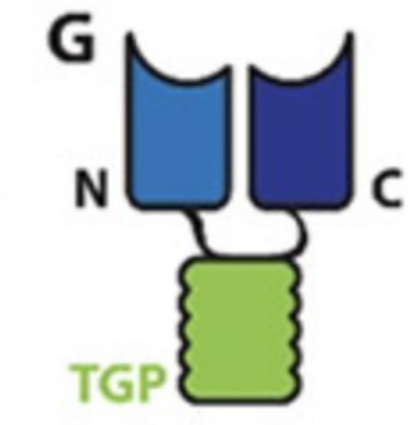

Figure 7. Example of nanobody-FP fusion of TGP between light and heavy chain antibodies adapted from Velappan et al.[28]

Many times a flow cytometer is used to detect the antibodies, as shown above, especially for gene and protein expression.[29] A flow cytometer is an instrument that can rapidly analyze single cells or particles as they flow past single or multiple lasers while suspended in a salt base buffer. Figure 8 shows how the samples flow down where the laser then analyzes the cell. Advancements to this instrument have been made by using multiple lasers to allow for multiple parameters and types of samples to be used.[29] There was a need to have more than one color of fluorescent protein for cell labeling.

It has been well established that alterations in the chromophore or local residues cause the chromophore's excitation and emission wavelengths to change. Changing the emission and excitation alters the color of the proteins, leading to the change in visible color. Figure 9 shows the different colors based on the emission and excitation wavelengths. This shift in emission and excitation from mutating the chromophore and local environment residues changes the charges

of residues, hydrogen bonding networks, and hydrophobic interactions that can lead to an emission shift of up to 40 nm.[30] Larger shifts in emission and excitation are due to differences in the covalent structure, as well as the extent of conjugation of the chromophore.[30] These mutations in the residues on or around the chromophore has led to a blue, cyan, and yellow version of GFP that is displayed in Figure 10.[3,4,25] To make a yellow version of GFP(YFP), histidine or tyrosine was incorporated under the chromophore, which leads to π stacking interaction which is displayed in Figure 10.[4] Additional rounds of mutations were needed for YFP to improve the pH stability, folding rate, expression temperature, and sensitivity to chloride ions.[31,32]

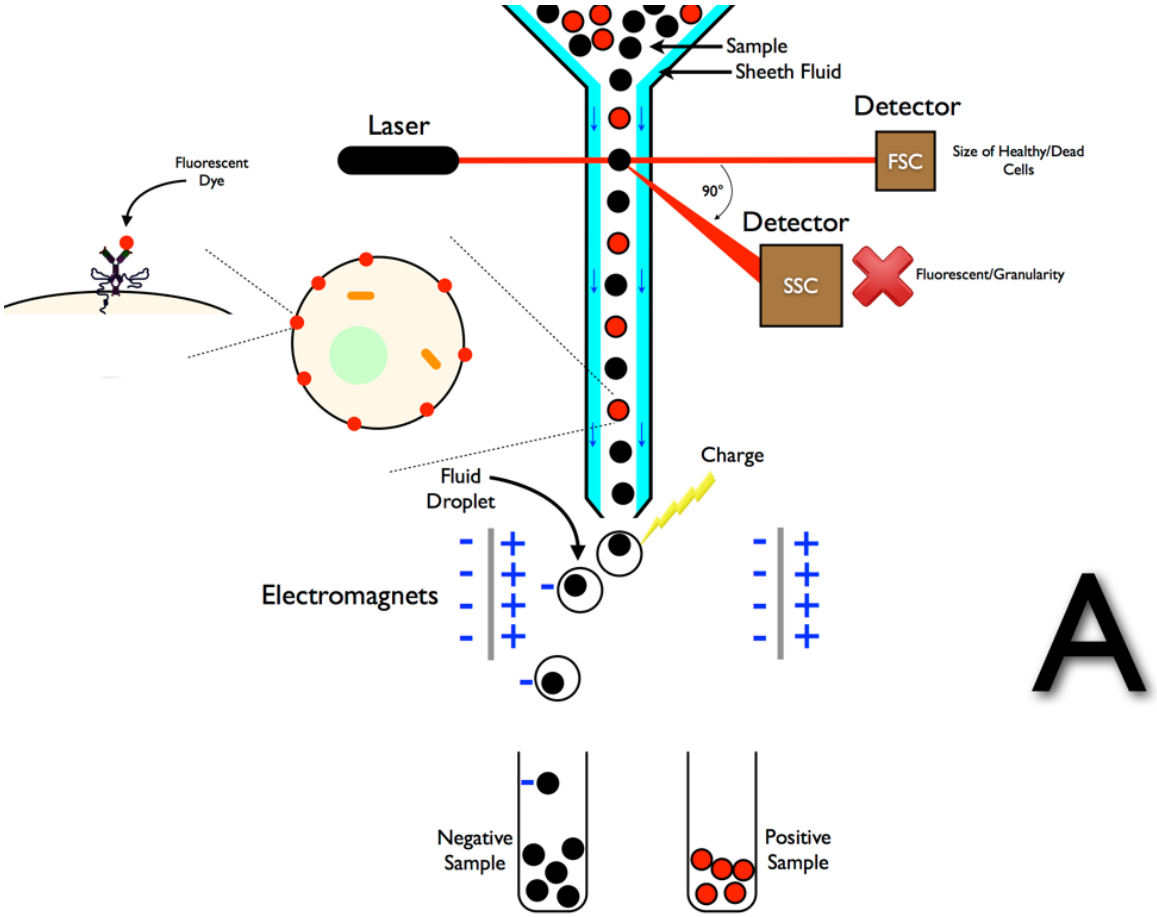

Figure 8. Example of how a flow cytometer works adapted from Sabban et al.[33] CC BY-SA 3.0 https://creativecommons.org/licenses/by-sa/3.0/, no changes were made.

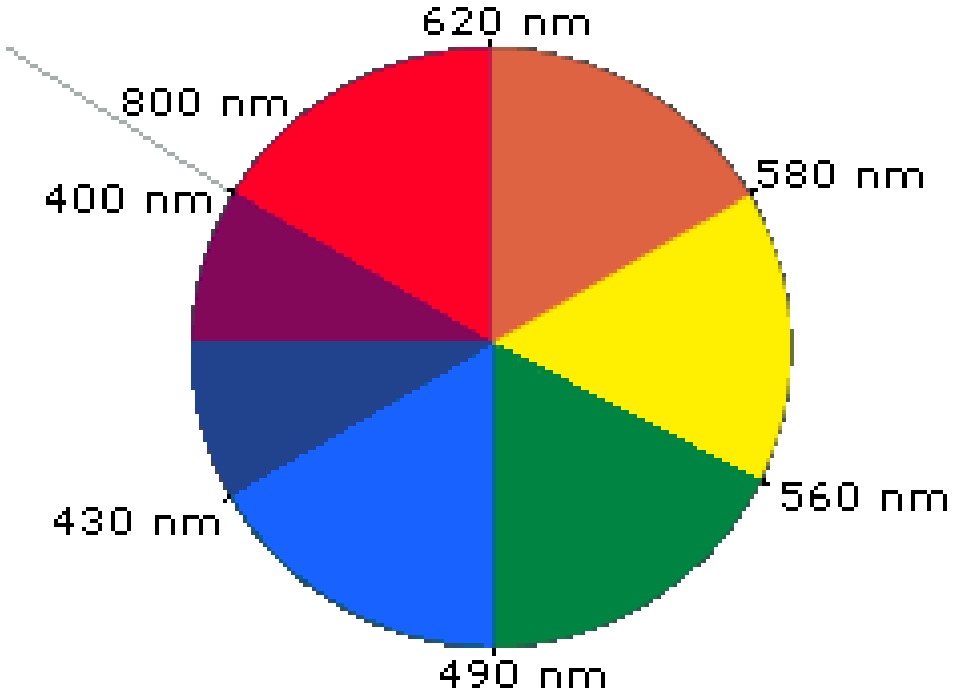

Figure 9. Example of a color wheel with the wavelengths of the primary colors adapted from MSU et al.[34]

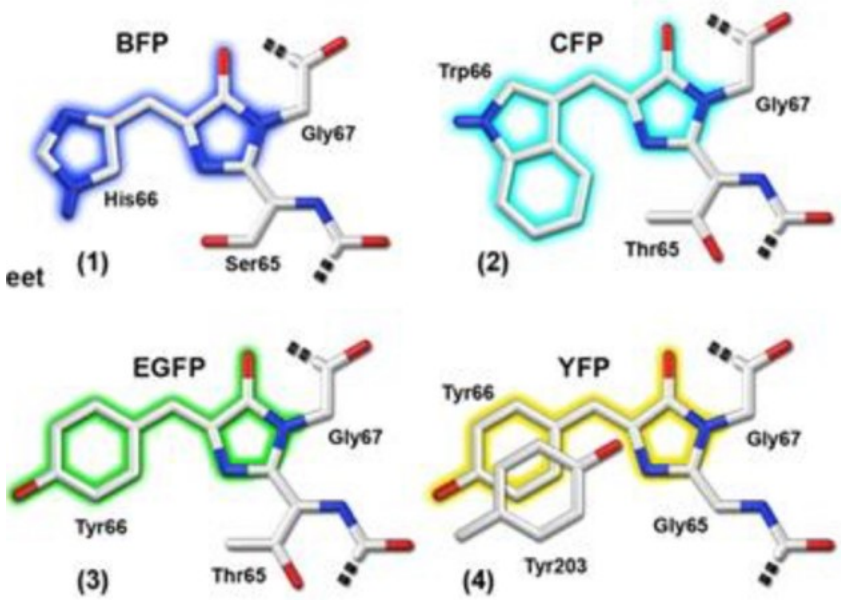

Figure 10. Examples of how the color of the fluorescent proteins changes based on mutations to or around the chromophore adapted from Shaner et al.[30]

The main goal of this research is to develop a yellow version of TGP. The π stacking interaction is already present with the chromophore and histidine 193 in TGP. Using site-directed mutagenesis to mutate histidine 193 to tyrosine leads to a yellow protein (YTP) that displays better thermostability and similar chemical and pH stability to TGP. Both GFP and the monomeric derivative mRFP1 from DsRed showed altered spectral characteristics when altering the first residue in the chromophore. One of the earliest mutations made to GFP was from mutating serine 65 to threonine, which improved the ionization of the chromophore phenol. This resulted in a single excitation peak at 489-490 nm.[3] DsRed protein mutation of glutamine at residue 66 led to changes in the excitation and emission wavelengths, this was followed with a series of yellow to red mFruit proteins.[25] Alterations to the hydrogen bonding network between the chromophore and the fluorescent protein is known to alter the spectral properties of fluorescent proteins.[35] With this in mind, alterations were made to both TGP and YTP by mutating the chromophore residue glutamine 66 to glutamate in both proteins making TGP-E and YTP-E. From crystallography of the TGP-E structure, it was determined that the glutamine 66 to glutamate mutation did alter the hydrogen bonding network by adding an additional hydrogen bond and decreasing another hydrogen bond's length, further stabilizing the proteins.

METHODS

Experimental

Site-Directed Mutagenesis of TGP. The TGP gene (synthetic protein) in the pETCK3 expression plasmid was provided by Los Alamos National Laboratory. Oligonucleotide primers (Table 1) were purchased from Thermo Fisher Scientific to mutate the histidine 193 to tyrosine and from glutamine 66 to glutamate. The YTP Q66E mutation was made by using TGP H193Y (YTP) to form a double mutant. The full sequence comparisons of TGP to mutant proteins are provided in Figure 11. Mutations were induced using the Agilent QuickChange II site-directed mutagenesis kit. Plasmid purification was then carried out using a GeneJet plasmid miniprep kit (Thermo Scientific). The purified plasmid was sequenced at ACGT, Inc to verify proper mutation.

Table 1. Primers used for site-directed mutagenesis

Mutation	Forward primer	Reverse primer
H193Y	CACGAGGTGGACTACCGCATTGA AATCCTG	CAGGATTTCAATGCGGTAGTCCA CCTCGTG
Q65E	CCAGCCTTCGAATACGGC	GCCGTATTCGAAGGCTGG

Expression and Purification of Protein. Proteins were expressed in *Escherichia coli* (*E. coli*) BL21(DE3) cells. A single colony was selected of each mutant and grown overnight in a 50 mL liquid Lennox broth (LB) with 50 µg/mL kanamycin at 37 °C. Next, 25 mL of overnight culture was added to 1 L of LB with 50 µg/mL kanamycin and grown at 37 °C until OD_{600} was greater than 0.4. Then, 1 mM IPTG was added to induce protein expression, and the temperature

was reduced to 30 °C. Finally, the *E. coli* cells were harvested by centrifugation at 5000 rpm for 10 minutes after 1 day of growth and stored at -80 °C. In addition, for the YTP and YTP-E, the volume of growth was doubled to 2 L in terrific broth media, and growth after induction was increased to 3 days at a lower temperature of 26 °C.

The proteins were extracted from the *E. Coli* cells by sonication on ice for 30 seconds at a time with a 30-second rest three times in lysis buffer (0.1 M Tris, pH 7.4, 10% glycerol, 0.3 M NaCl), then centrifuged at 20,000 rpm for 20 minutes. The lysate was purified by affinity chromatography NINTA (Gold Biotechnology). Proteins were washed with wash buffer (0.1 M Tris pH 7.4, 50 mM NaCl, 10 mM imidazole, 10% glycerol), then eluted with elution buffer (0.1 M Tris pH 7.4, 200 mM imidazole, 10% glycerol, 100 mM NaCl). Proteins were further purified by ion exchange chromatography using DEAE column (Bio-Rad) and eluted in elution buffer (0.1 M Tris pH 7.4, 0.5 M NaCl, 10% glycerol). SDS- page gels were used to determine that were present at 28 kDa where the protein is to be expected and to verify purity.

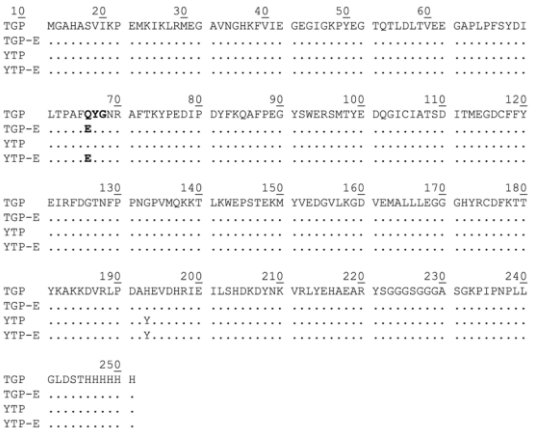

Figure 11. Protein sequence alignment of TGP-E, YTP, and YTP-E to TGP.

Measurement of Ultraviolet (UV) and Visible Absorption spectra. The absorbance spectra of all TGP and mutant purified proteins were measured using a Shimadzu UV- 2101 PC

spectrometer from 700 to 250 nm with a slit width of 2.0 nm. The purified protein concentrations were determined by using the 280 nm peak using Beer's law. The emission peaks of the proteins were also measured using a PerkinElmer LS 55 fluorescence spectrometer with excitation at 470 nm for TGP-E and emission scan from 490 nm - 600 nm and excitation at 480 nm for YTP-E with emission scan from 500 nm to 600 nm.

Thermostability Measurements. Thermostability measurements for TGP, TGP-E, YTP, and YTP-E were obtained using an RT-PCR (QuantStudio 6 Applied Biosystems). The measurements were performed using 3.75 pmol of protein to assay buffer (0.1 M Tris, pH 7.4, 20 mM $MgCl_2$) in a 96-well PCR plate. The measurements were initially recorded at 25 °C before temperature ramping to either 90 or 60 °C where fluorescent measurements were made once per minute for an hour at a ramp rate of 1.6 °C/S. The measurements were made using a FAM filter, which has 470 ± 15 nm excitation and 520 ± 15 nm emission. For the analysis, the percent fluorescences remaining was normalized to the fluorescent value at 25 °C initially measured. For unfolding and refolding, the same setup was used where it was first measured at 25 °C then ramped up to 99 °C at a rate of 0.9 °C/min, and fluorescences were measured every 1.7 seconds. Then the temperature was quickly decreased rapidly to 25 °C and the fluorescence was measured every 30 seconds for an hour. The recovery ramping was repeated three more times for a total of four cycles with at least four biological replicate samples.

Chemical Denaturation. The purified fluorescent protein at 3.75 pmol was diluted in assay buffer (0.1 M Tris HCl pH 7.4, 20 mM $MgCl_2$) into guanidinium HCl (Gdm HCl) with a range of concentrations from 0 to 8 M. The fluorescences were measured on a spectraMax M5 plate reader. The excitation and emission wavelengths were set to 490 nm and 508 nm for TGP and TGP-E and the excitation at 510 nm with the emission at 525 nm for YTP and YTP-E. To

determine when equlibrlibrum was reached at the concentration of 0 to 8 M Gdm measurements were made after 1 hour, 5 days, and 10 days at room temperature. The day 5 and 10 measurements were relatively proportional to each other indicating they have reached equilibrium. The fluorescence was normalized against the 0 M Gdm concentration to ensure equilibrium was reached and to analyze the data the 10-day incubation time was used. All experiments were completed with 4 biological replicates (from two different protein preps).

Sensitivity to pH. The purified protein was diluted 15-fold into 0.1 M glycine-phosphate-citrate buffers with 0.1 M NaCl at varying pH levels from 3 to 10 and incubated at room temperature for one hour. The fluorescence was measured on a SpectraMax M5 plate reader with the same excitation and emission as the chemical denaturant assay. Fluorescence was normalized to the pH with the highest fluorescence for each protein.[6] The YTP-E protein had a different maximum value for each trial run, showing no consistent 100% fluorescence when graphed. Each experiment was performed using 5 biological replicates.

Crystallography of TGP Varients. The TGP-E protein crystals were grown via the hanging vapor drop diffusion method where 1 µL of purified protein was concentrated around 20 mg/mL each time with 1 µL of the various well solutions displayed in Table 2. The crystal plates were set up in a clean hood to prevent any contamination. The crystals grew at 22 ° C where they would consistently develop crystals approximately 30 days after being plated. The TGP-E crystals would only grow if the wells were greased with immersion oil. When using vacuum grease they would tend to develop at a slower rate or not at all. On the other hand, the YTP-E crystals would grow best when using vacuum grease and consistently produce crystals, but if immersion oil was used to seal wells they would develop very slowly or not at all. Overall, if the TGP-E and YTP-E were not provided with their preferred sealant they showed less diffraction

than crystals that were grown in their preferred sealant. Something else to note is that the YTP-E crystals consistently formed a precipitate, despite how pure the protein prep was making it difficult to obtain and view the crystals.

Table 2. Crystal screening Conditions for TGP variant proteins.

	1	2	3	4	5	6
A	0.15 M Magnesium chloridehexa-hydrate 0.1 M TRIS hydrochloride pH 8.5 30 % PEG 4000	0.2 M Magnesium chloridehexa-hydrate 0.1 M TRIS hydrochloride pH 8.5 30 % PEG 4000	0.25 M Magnesium chloridehexa-hydrate 0.1 M TRIS hydrochloride pH 8.5 30 % PEG 4000	0.3 M Magnesium chloridehexa-hydrate 0.1 M TRIS hydrochloride pH 8.5 30 % PEG 4000	0.35 M Magnesium chloridehexa-hydrate 0.1 M TRIS hydrochloride pH 8.5 30 % PEG 4000	0.4 M Magnesium chloridehexa-hydrate 0.1 M TRIS hydrochloride pH 8.5 30 % PEG 4000
B	0.15 M Magnesium chloridehexa-hydrate 0.1 M TRIS hydrochloride pH 8.5 32.5 % PEG 4000	0.2 M Magnesium chloridehexa-hydrate 0.1 M TRIS hydrochloride pH 8.5 32.5 % PEG 4000	0.25 M Magnesium chloridehexa-hydrate 0.1 M TRIS hydrochloride pH 8.5 32.5 % PEG 4000	0.3 M Magnesium chloridehexa-hydrate 0.1 M TRIS hydrochloride pH 8.5 32.5 % PEG 4000	0.35 M Magnesium chloridehexa-hydrate 0.1 M TRIS hydrochloride pH 8.5 32.5 % PEG 4000	0.35 M Magnesium chloridehexa-hydrate 0.1 M TRIS hydrochloride pH 8.5 32.5 % PEG 4000
C	0.15 M Magnesium chloridehexa-hydrate 0.1 M TRIS hydrochloride pH 8.5 35 % PEG 4000	0.2 M Magnesium chloridehexa-hydrate 0.1 M TRIS hydrochloride pH 8.5 35 % PEG 4000	0.25 M Magnesium chloridehexa-hydrate 0.1 M TRIS hydrochloride pH 8.5 35 % PEG 4000	0.3 M Magnesium chloridehexa-hydrate 0.1 M TRIS hydrochloride pH 8.5 35 % PEG 4000	0.35 M Magnesium chloridehexa-hydrate 0.1 M TRIS hydrochloride pH 8.5 35 % PEG 4000	0.4 M Magnesium chloridehexa-hydrate 0.1 M TRIS hydrochloride pH 8.5 35 % PEG 4000
D	0.15 M Magnesium chloridehexa-hydrate 0.1 M TRIS hydrochloride pH 8.5 37.5 % PEG 4000	0.2 M Magnesium chloridehexa-hydrate 0.1 M TRIS hydrochloride pH 8.5 37.5 % PEG 4000	0.25 M Magnesium chloridehexa-hydrate 0.1 M TRIS hydrochloride pH 8.5 37.5% PEG 4000	0.3 M Magnesium chloridehexa-hydrate 0.1 M TRIS hydrochloride pH 8.5 37.5 % PEG 4000	0.35 M Magnesium chloridehexa-hydrate 0.1 M TRIS hydrochloride pH 8.5 37.5 % PEG 4000	0.4 M Magnesium chloridehexa-hydrate 0.1 M TRIS hydrochloride pH 8.5 37.5 % PEG 4000

Once the crystals were developed to a size that would fit in a 0.1 nm loop, they were selected and transferred to a solution of 3:1 mother well solution to glycerol. The crystals were

then flash-frozen in the cryo stream at 100 K and the diffraction was collected at 100 K using a Rigaku XtaLab Synergy-S. The data was collected using CrysAlis^{Pro} software. Molecular replacement was performed on TGP-E using monomeric Azami Green (mAG) as the sequence model (PDB 3ADF) and the refinement was performed using CCP4 and the model building was done in COOT.

RESULTS

Most of the research presented has been published in "Engineering a Yellow Thermostable Fluorescent Protein by Rational Design", https://doi.org/10.1021/acsomega.2c05005

TGP-E Mutants

With the pETCk3 TGP used as the initial material, a tyrosine 193 mutation was made by site-directed mutagenesis leading to a red-shifted protein (YTP). After developing the red-shifted protein another mutation was made; located on the chromophore by mutating the glutamine 66 to glutamate. This Q66E mutation was incorporated into TGP and YTP to TGP-E and YTP-E. The mutations were sent off to ACGT to have DNA sequencing done to verify the mutations. Once the mutations were verified we were able to proceed with expression and purification.

Protein Expression and Purification

The proteins were expressed in BL21 (DE3) cells. The purification process is stated in the methods. The initial starting culture was 50 mL per 1 L scale up with 1 day of expression. The initial expression provided high yield for TGP-E but did not provide a very high yield for YTP-E. Several Improvements were made. The first was doubling the large-scale growth from 1 to 2 liters, second was lowering the temperature to 26 °C, and third was increasing the expression time to three days which seemed to slightly improve concentration. The last improvement made was to double the starter culture volume from 50 to 100 mL. Once YTP-E was purified on a nickel and DEAE column the concentration averaged 15.6 μM compared to the average concentration of 5 μM prior to improvements. TGP-E and YTP-E both were run on an

SDS-PAGE gel alongside TGP and YTP. TGP-E showed to be pure with no predominate bands other than the one at 28 KDa (Figure 12) while YTP-E had quite a few bands other than the 28 KDa demonstrating a lack of purity.

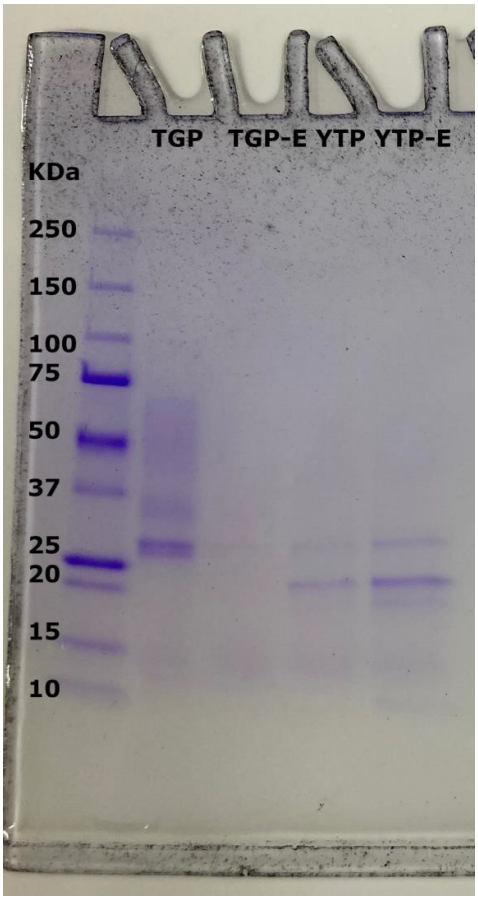

Figure 12. SDS-PAGE gel of TGP, TGP-E, YTP, and YTP-E.

Fluorscent Absorbtions of Proteins

Once the purification was complete the protein's absorbances were measured to determine the absorption and emission of the proteins. From Figure 2, one can see the excitation and emission for TGP, TGP-E, YTP, and YTP-E. The determined excitation of YTP is at a wavelength of 513 nm and the emission is at 522 nm which is relatively similar to other yellow fluorescent proteins (Table 3). YTP-E has the same excitation wavelength as YTP but the

emission is slightly shifted to a higher wavelength of 526 nm. While a similar occurrence occurs for TGP and TGP-E, where they have the same excitation wavelength at 513 nm (Table 3). The emission of TGP is slightly red-shifted or at a higher wavelength than TGP-E (Figure 13). The emission of TGP is at 507 nm and TGP-E is at 509 nm (Table 3). Overall, the mutation Q66E redshifts both YTP and TGP.

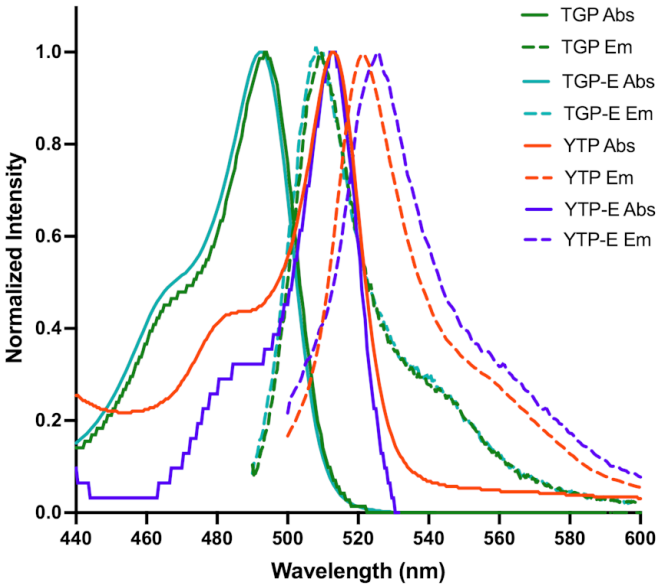

Figure 13. Absorbance and emission spectra for TGP, TGP-E, YTP, and YTP-E; the intensity is normalized to maximal chromophore absorption or emission.

Table 3. The excitation and emission wavelengths for TGP, TGP-E, YTP, and YTP-E.

Protein	Excitation λ_{max} (nm)	Emission λ_{max} (nm)
TGP	493	507
TGP-E	493	509
YTP	513	522
YTP-E	513	526

pH Stability Assays

The pH stabilities of the proteins were determined and compared by measuring the changes in fluorescence of the proteins with varying pH. The pH sensitivity for the mutants was similar to TGP, the pK_a value for TGP was 6.7 with 95% confidence between 6.5 to 6.9 (Figure 14A). The pK_a values for YTP of 6.7 with 95% confidence between 6.5 to 7.0 and TGP-E at 6.6 with 95% confidence between 6.4 to 6.9 (Figure 14A). YTP-E altogether lacks pH sensitivity (displayed by the lack of a sigmodal curve having a low and a high percent fluorescence) that the other three proteins have (Figure 14B). It is also worth noting that YTP does seem to have higher fluorescence at lower pH than TGP and TGP-E (Figure 14A). While it may also seem that TGP-E does better at higher pHs than TGP-E and YTP. Once TGP is at a pH of 10, the percent fluorescence drops to 49 ± 5 %. This drops significantly compared to the other two proteins. Due to the significant drop in fluorescence of TGP, the data point was not included in Figure 14A.

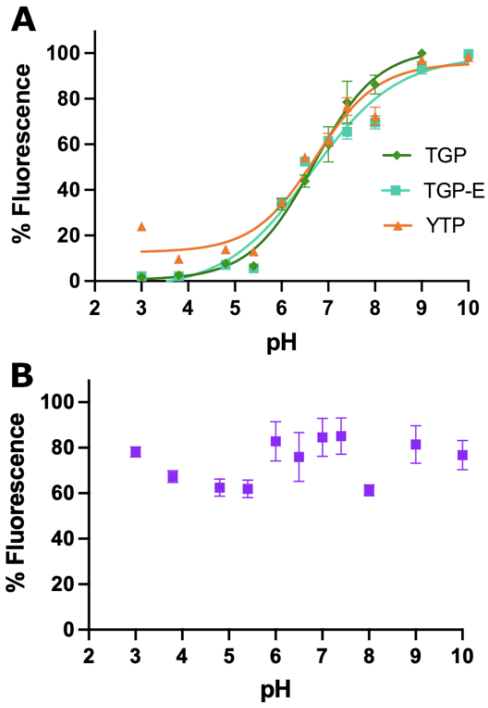

Figure 14. (A) pH titration of TGP, TGP-E, and YTP. (B) pH titration of YTP-E.

Thermal Denaturation and Refolding Assays

The unfolding and refolding of TGP, TGP-E, YTP, and YTP-E were determined with the use of an RT-PCR instrument. A FAM filter was used and set to 470 ± 15 nm excitation and 520 ± 15 nm emission. In order to accurately depict the unfolding and refolding of the proteins were all maintained at the same concentration of 3.75 pmol for every RT-PCR experiment. The proteins were diluted into the assay buffer, then the fluorescence was measured in real-time. For the unfolding experiments, the temperature started out at 25 °C and then slowly ramped up at a rate of 0.9 °C/min to 99 °C measuring fluorescence every 1.7 seconds. The refolding was determined by rapidly bringing the proteins back down to 25 °C at a ramp rate of 2.32 ° C/sec and held for one-hour recording fluorescences every 30 seconds. The combination of unfolding and refolding experiments was run together and repeated 3 more times with a total of 4 cycles (Figure 15). Each protein graph in Figure 15 has each cycle plotted on the same graph to show the protein's ability to recover along with the protein's heating cycle. The stability of YTP and YTP-E are quite pronounced as they both return to their preheated levels of fluorescence (Figure 15B, D). YTP and YTP-E both also never reached zero percent fluorescence during the heating process to 99 °C. YTP maintained a 33% fluorescence during its first cycle at 99 °C and during cycles two, three, and four it maintained a fluorescence of 45% (Figure 15B). Something else to note is that YTP started out with more than 100% fluorescence during cycles two, three, and four. This indicates that it has more fluorescence than cycle one initially started with. YTP-E maintained 40% fluorescence for all four cycles while heating to 99 °C and maintained close to 100 % recovery after heating during all four cycles (Figure 4D). While YTP and YTP-E maintain their fluorescence, the same can not be said about TGP and TGP-E. They only maintained 1 to 5 % fluorescence during heating at 99 °C during all four cycles (Figure 15A, C). TGP only recovered 30% of its fluorescence after heating during the first cycle, after the second 18%, for

the third 12 %, and after the fourth cycle only 9% of fluorescence was recovered (Figure 15A). While TGP-E did do slightly better at recovery it was not comparable to YTP and YTP-E (Figure 15C). After TGP-E's first cycle, 45% of fluorescence was recovered, for the second cycle 34%, in the third 28%, and in the fourth cycle recovered 24% fluorescence (Figure 15C).

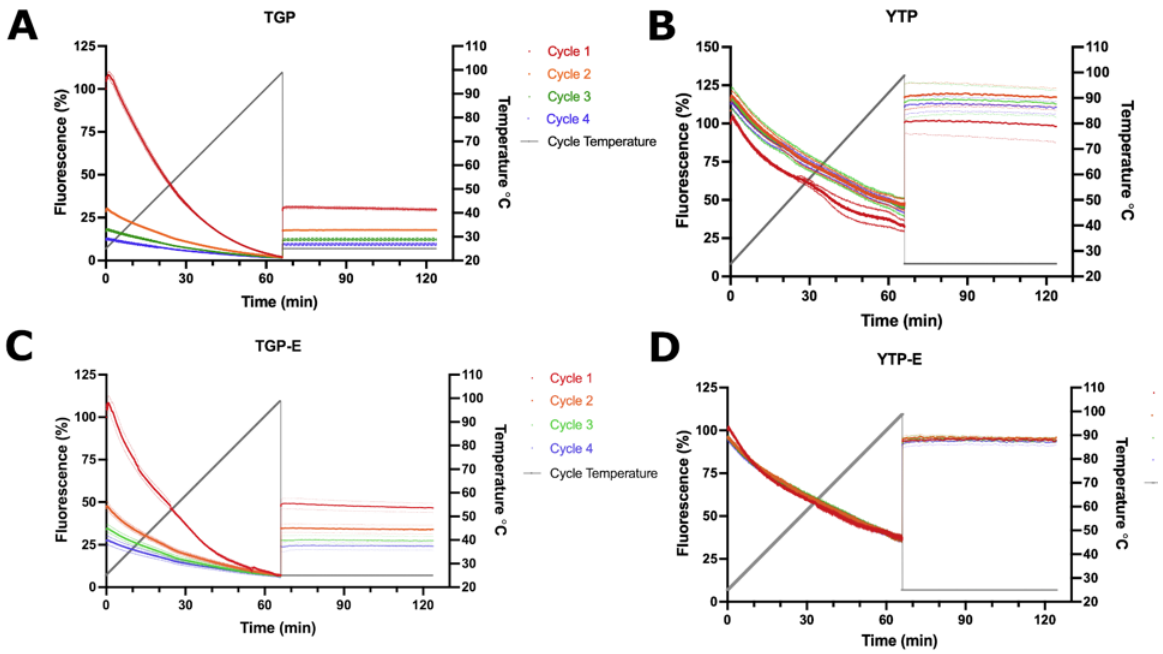

Figure 15. (A) TGP, (B) YTP, (C) TGP-E, and (D) YTP-E were assayed for unfolding and recovery(refolding) with four cycles.

Thermostability Assay

The thermal stability of TGP, TGP-E, YTP, and YTP-E was measured at 60 °C and 90 °C and held for one hour (Figure 16). Like the unfolding and refolding experiments, all the proteins were concentrated to 3.75 pmol and then diluted into assay buffer. The data is normalized by the initial fluorescent reading at 25 °C before heating began. For the thermostability, there was an initial drop in fluorescence once heating began and then the proteins equilibrate (Figure 16).

YTP and YTP-E are similar, with their ability to unfold and their recovery appearing to be very stable. Both only dropped down to 60% fluorescence, then after one hour rose back to almost 70% at 60 °C (Figure 16A). At 60 °C YTP-E is slightly more stable than YTP once it has the chance to equilibrate. While at 90 °C YTP and YTP-E, both equilibrate close to 60% fluorescence. YTP does seem to be slightly more stable than YTP-E at 90°C (Figure 16B). Unlike YTP and YTP-E where they were both similar at 60 and 90 °C, TGP and TGP-E are only similar in fluorescence at 60 °C and very different at 90 °C (Figure 16). At 60°C TGP and TGP-E both lose fluorescence to around 30%. At 90 °C, TGP-E is significantly less stable where there is only 10% left of the initial fluorescence after an hour, while 30% of TGP initial fluorescence remains (Figure 16). It is worth noting that TGP-E is the only protein to have such a significant loss of fluorescence within the first 20 minutes of heating.

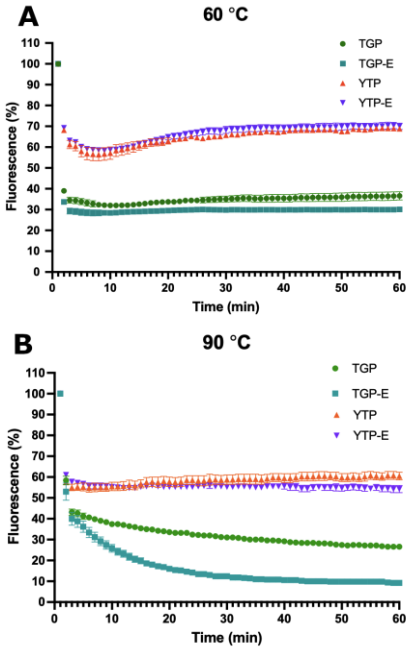

Figure 16. (A) The thermostability of TGP, TGP-E, YTP, and YTP-E at 60 °C. (B) The thermostability of TGP, TGP-E, YTP, and YTP-E at 90°C.

Chemical Denaturing Assay

The protein's stability was further characterized by chemical denaturing, using various concentrations of Gdn HCl from 0 to 8 M to characterize their equilibrium that was reached after 10 days of incubating at room temperature (Figure 17). The C_m for TGP was 6.0 M with a 95% confidence interval of 5.6 to 6.2. TGP-E's C_m was 5.0 M with a 95% confidence interval of 4.7 to 5.4 and YTP was 4.2 M confidence interval of 4.0 to 4.3. Between TGP, TGP-E, and YTP: TGP had the highest chemical denaturing midpoint, indicating that it took higher concentrations to reach equilibrium and is more stable than the other three proteins. Despite TGP being more stable, it is noteworthy that TGP-E was not fully unfolded at 8 M of Gdn HCl unlike TGP and YTP (Figure 17A). On the other hand, YTP-E appeared to have no trend of unfolding with the increasing Gdn HCl concentration (Figure 17B). In fact, YTP-E had an overall loss of 20% which can be seen in Figure 17B. This lack of denaturing in its tertiary structure indicates that the protein is very stable and can be used in more unhabitable environments.

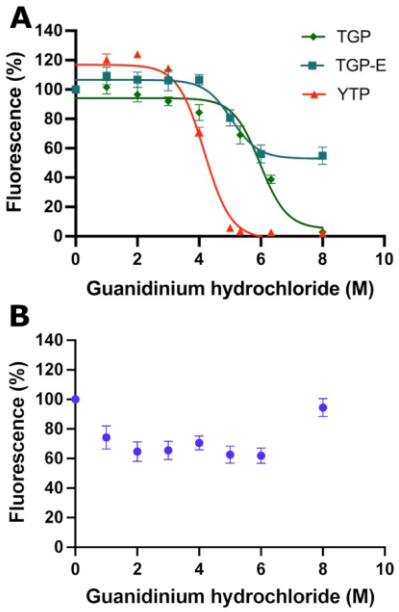

Figure 17. (A) Equilibrium unfolding plot for TGP, TGP-E, and YTP. (B) Equilibrium unfolding plot of YTP-E.

Crystallography

We obtained consistent protein crystals of TGP-E with the crystal conditions noted in the methods section. Most crystals appeared to have a rod shape with a clear green color - Figure 18. The crystals would appear roughly around the two-week mark. After screening over fifty crystals, we were able to obtain TGP-E's crystal that diffracted. This can be seen in Figure 19 and the diffraction pattern in Figure 20. The TGP-E crystal structure was obtained at a resolution in the range of 20.42 to 2.00 Å and found to have 2 molecules in the asymmetric unit of symmetry based on the structure's Matthew's coefficient calculated using CCP4 (Table 4). The TGP-E crystal was found to belong to space group P1 with two molecules in the asymmetric units. Further collection and analysis data are presented in Table 4. The structure was solved by molecular replacement using mAG as a search model in CCP4. Once molecular replacement was complete, the structure was refined using Coot to determine the final model of TGP-E. This process involved interactive rounds of model building in COOT followed by refinement in Refmac in CCP4. Refinement statistics are in Table 4. The structure is similar to TGP, with a typically conserved beta-barrel protein with the chromophore in the center (Figure 21).

Figure 18. TGP-E crystal after roughly two weeks of growing in crystal plate.

Figure 19. The TGP-E crystal that the structure was collected on captured in the loop.

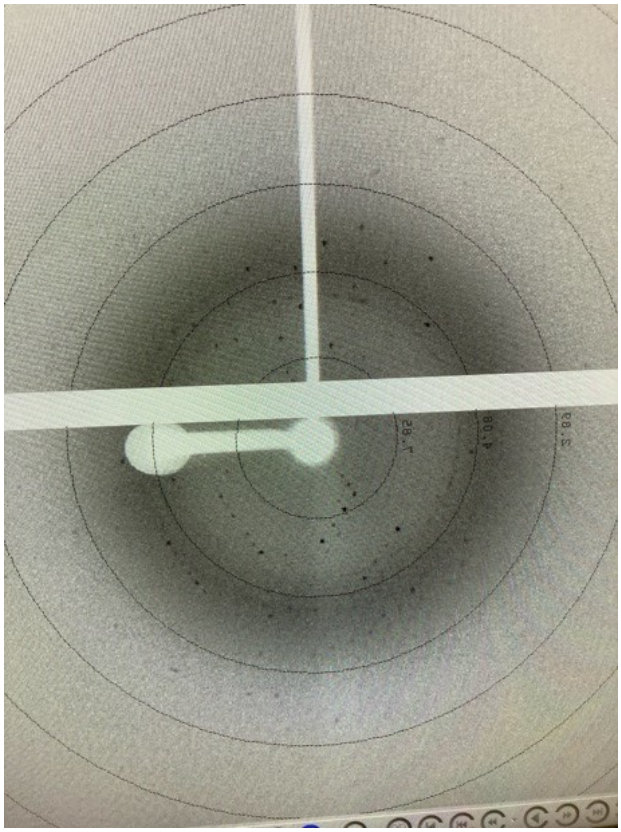

Figure 20. TGP-E diffraction that was collected on the X-Ray diffractometer.

Table 4. TGP-E refinement statistics.

	TGP-E
Resolution range (Å)	20.42 - 2.00
Space group	P1
Unit-cell parameters (Å,°)	38.74 49.06 59.11 78.55 72.08 71.41
No. total refelctions	
Overall	149158
Outershell	10544
No. unique reflections	26322
Overall	26322
Outershell	1957
Multiplicity	
Overall	5.7
Outershell	5.4
Completeness (%)	
Overall	99.9
Outershell	100
Rpim (all I+ & I-)	
Overall	0.092
Outershell	0.412
Refinement Statistics	
R value	0.198
R Free Value	0.246
Ramachandran favored (%)	97.3

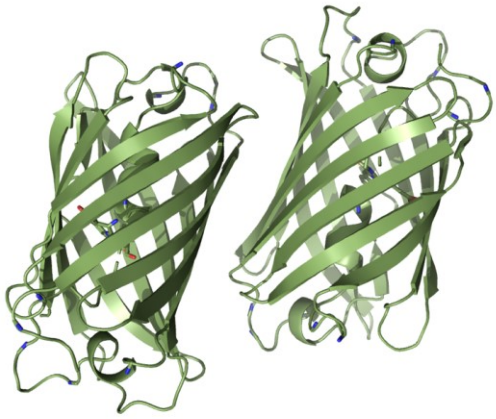

Figure 21. TGP-E structure after refinement.

Although we have not obtained the YTP-E structure yet, we have obtained diffraction that was predicted to be close to a high enough resolution to collect on. YTP-E crystals grow in the same condition as TGP-E crystals, differing in their preference for sealing with vacuum grease. They appear after two weeks of growth also with a rod-like appearance (Figure 22). We have screened over 100 YTP-E crystals so far. The best diffracting crystal had unit cell dimensions of 45.22 Å 136.64 Å 77.98 Å 89.97 Å 96.03 Å 90.00 Å and was predicted to be in space group P2. YTP-E's best diffracting crystal was estimated to diffract to 3.17 Å resolution; the diffraction pattern can be seen in Figure 23.

Figure 22. YTP-E crystal while on crystal plate.

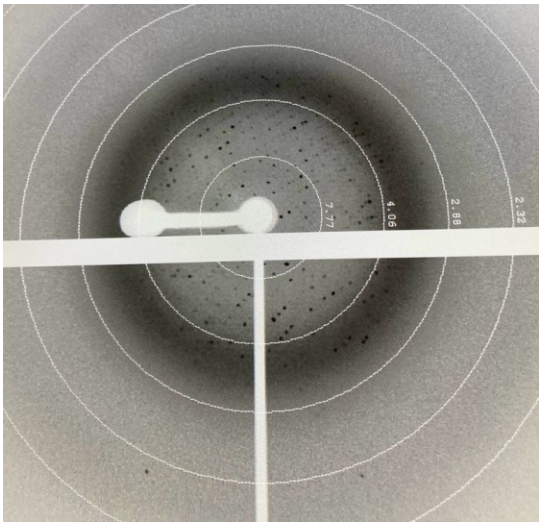

Figure 23. The diffraction pattern of the best diffracted YTP-E crysta

DISCUSSION

A yellow mutant was formed by using site-directed mutagenesis to incorporate a H193Y mutation below the chromophore. The yellow mutation leads to a shift in the excitation wavelength to 513 nm and emission to 522 nm. The tyrosine was shown to also shift GFP yellow when mutated in a similar location.[31,36] Both TGP and YTP were mutated to a glutamate 66 from glutamine on the chromophore in order to alter the hydrogen bonding networks near the chromophore. The crystal structure of TGP-E allowed us to see how the hydrogen bonding network changed. The mutation of glutamate to TGP-E allowed for an additional hydrogen bond to the backbone and a shorter hydrogen bond length of 2.8 Å bond than TGP which had a bond length of 3.0 Å (Figure 24). The bond also has an alternative conformation stacked on top of each other in TGP-E, likely helping with the stronger bonding. The shorter bond is overall due to the carbonyl being protonated. This is due to the carbonyl being located in a hydrophobic cage.[37] This closer hydrogen bond likely brought the chromophore closer to the backbone allowing for the additional hydrogen bond to form. The addition of the hydrogen bond's additional stability explains why TGP-E has more stable properties than TGP.

All of the mutants were sequenced and verified, then expressed in BL21 (DE3) cells, purified by affinity and ion exchange chromatography, and then characterized. Notably, neither the pH nor the glutamate mutation significantly improved TGP. For the pH stability, it seems the mutant was only slightly more stable at higher pHs. While the chemical denaturing TGP-E mutant did follow a similar sigmoidal curve as the non-mutant, the mutant did show a slightly higher fluorescence at higher concentrations of Gdn HCl and maintained 60% fluorescence at 8 M Gdn HCl - a substantial improvement over TGP. However, the mutation improvement on YTP

was even more significant. The mutant showed a complete lack of pH sensitivity (Figure 14B) and show no trend of unfolding or significant loss of fluorescence during chemical denaturing (Figure 17B). The glutamate mutation in TGP-E had a significant effect on the percent fluorescence recovery. The TGP mutant recovered a higher percent of fluorescence than TGP after being heated to high temperatures for a prolonged period of time, roughly 10 % higher for all 4 runs (Figure 15A&C). While the mutation did improve the percent recovery, it did not improve the overall thermal stability of the protein. This shows us that TGP-E has a higher percent recovery, but TGP maintains its fluorescence better at prolonged high temperatures (Figure 16A&B). YTP-E did significantly improve the percent recovery compared to YTP. The percent recovery for YTP-E stayed around 90% fluorescence for all four runs consistently while YTP lost more fluorescence during each run (by the fourth run only recovering around 80% fluorescence (Figure 15B&D). However, YTP-E did not significantly improve thermal stability. While at 60 °C YTP-E was slightly more stable than YTP they both recovered fluorescence around 60%(Figure 16 A). While at 90 °C YTP showed higher stability than YTP-E with roughly 10 % higher recovery (Figure 16A).

In conclusion, the one additional mutation, Q66E into TGP, produced TGP-E, a green thermal protein that showed increased chemical stability and improved percent recovery after being heated to high temperatures. Additionally, we developed a yellow thermal protein based on TGP with and without the Q66E mutation. Both of the yellow proteins are very thermal stable and have an excellent percent recovery of fluorescense. The YTP-E protein showed better percent recovery and was shown to have better pH and chemical stability. YTP-E is an excellent choice to be used in experiments that require lower pH such as use with acidic organelles like lysosomes or uses at higher temperatures with thermophilic organisms. The future direction for

this project would be to obtain the crystal structure of YTP-E which is currently underway. The crystal structure of YTP-E would be able to give insight into why its properties have improved as well as help with the future direction of engineering these thermostable fluorescent proteins.

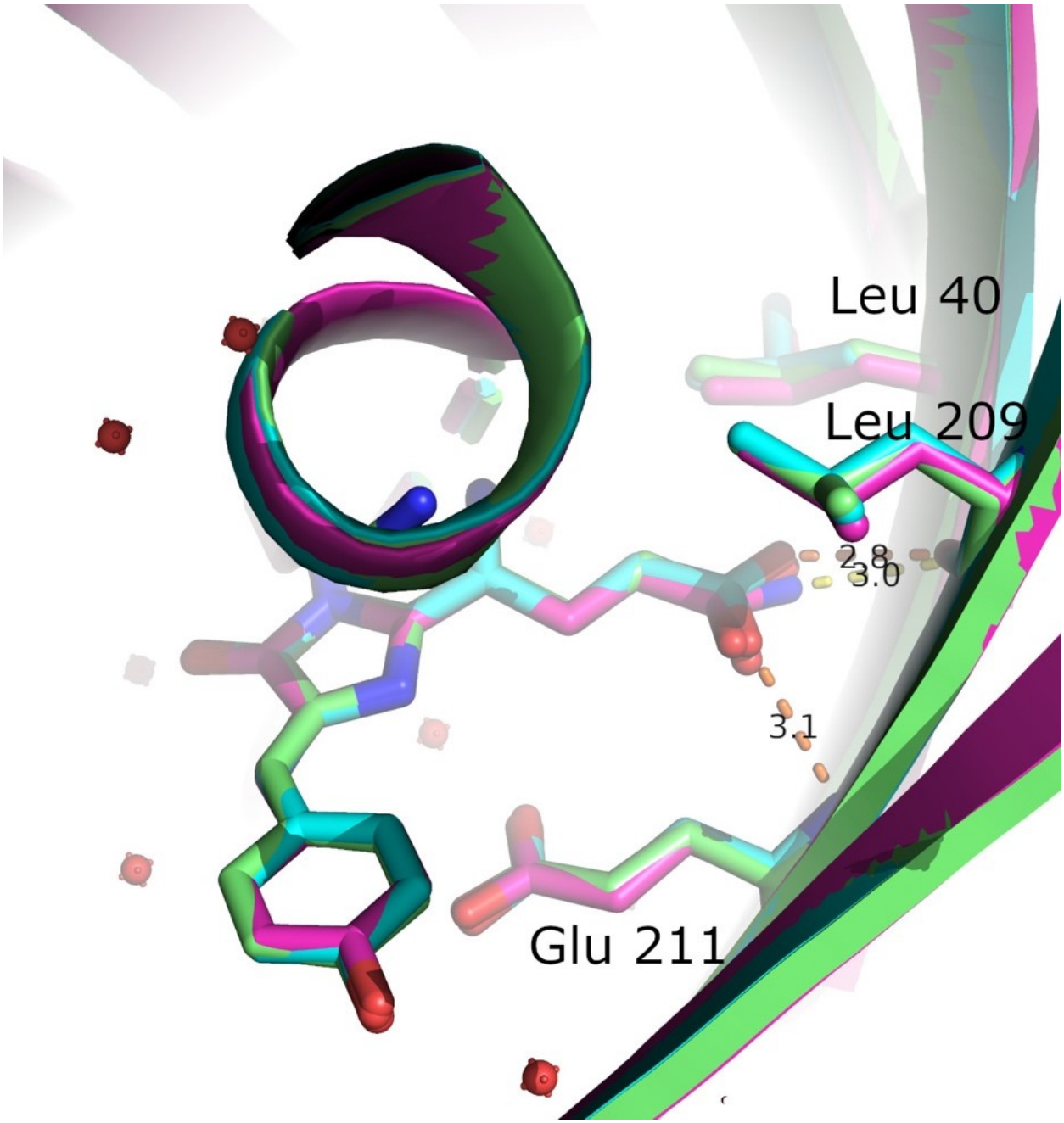

Figure 24. The Hydrogen bonding of TGP and TGP-E; TGP-E subunit B is blue, TGP-E subunit A is pink, TGP is labeled green the hydrogen bonds of TGP-E subunits are orange and TGP's are yellow**.**

REFERENCES

(1) Shimomura, O.; Johnson, F. H.; Saiga, Y. Extraction, Purification and Properties of Aequorin, a Bioluminescent Protein from the Luminous Hydromedusan,Aequorea. *J. Cell. Comp. Physiol.* **1962**, *59* (3), 223–239. https://doi.org/10.1002/jcp.1030590302.

(2) Chalfie, M.; Tu, Y.; Euskirchen, G.; Ward, W. W.; Prasher, D. C. Green Fluorescent Protein as a Marker for Gene Expression. *Science* **1994**, *263* (5148), 802–805. https://doi.org/10.1126/science.8303295.

(3) Tsien, R. Y. The Green Fluorescent Protein. *Annu. Rev. Biochem.* **1998**, *67* (1), 509–544. https://doi.org/10.1146/annurev.biochem.67.1.509.

(4) Ormö, M.; Cubitt, A. B.; Kallio, K.; Gross, L. A.; Tsien, R. Y.; Remington, S. J. Crystal Structure of the ***Aequorea Victoria*** Green Fluorescent Protein. *Science* **1996**, *273* (5280), 1392–1395. https://doi.org/10.1126/science.273.5280.1392.

(5) Shcherbakova, D. M.; Verkhusha, V. V. Chromophore Chemistry of Fluorescent Proteins Controlled by Light. *Current Opinion in Chemical Biology* **2014**, *20*, 60–68. https://doi.org/10.1016/j.cbpa.2014.04.010.

(6) Aliye, N.; Fabbretti, A.; Lupidi, G.; Tsekoa, T.; Spurio, R. Engineering Color Variants of Green Fluorescent Protein (GFP) for Thermostability, PH-Sensitivity, and Improved Folding Kinetics. *Appl Microbiol Biotechnol* **2015**, *99* (3), 1205–1216. https://doi.org/10.1007/s00253-014-5975-1.

(7) Cava, F.; de Pedro, M. A.; Blas-Galindo, E.; Waldo, G. S.; Westblade, L. F.; Berenguer, J. Expression and Use of Superfolder Green Fluorescent Protein at High Temperatures in Vivo: A Tool to Study Extreme Thermophile Biology. *Environ Microbiol* **2008**, *10* (3), 605–613. https://doi.org/10.1111/j.1462-2920.2007.01482.x.

(8) Holder, A. N.; Ellis, A. L.; Zou, J.; Chen, N.; Yang, J. J. Facilitating Chromophore Formation of Engineered Ca2+ Binding Green Fluorescent Proteins. *Archives of Biochemistry and Biophysics* **2009**, *486* (1), 27–34. https://doi.org/10.1016/j.abb.2009.03.016.

(9) Habuchi, S.; Ando, R.; Dedecker, P.; Verheijen, W.; Mizuno, H.; Miyawaki, A.; Hofkens, J. Reversible Single-Molecule Photoswitching in the GFP-like Fluorescent Protein Dronpa. *Proc. Natl. Acad. Sci. U.S.A.* **2005**, *102* (27), 9511–9516. https://doi.org/10.1073/pnas.0500489102.

(10) Crivat, G.; Taraska, J. W. Imaging Proteins inside Cells with Fluorescent Tags. *Trends in Biotechnology* **2012**, *30* (1), 8–16. https://doi.org/10.1016/j.tibtech.2011.08.002.

(11) Jensen, E. C. Use of Fluorescent Probes: Their Effect on Cell Biology and Limitations. *Anat Rec* **2012**, *295* (12), 2031–2036. https://doi.org/10.1002/ar.22602.

(12) Ghosh, A.; Sarkar, S.; Banerjee, S.; Behbod, F.; Tawfik, O.; McGregor, D.; Graff, S.; Banerjee, S. K. MIND Model for Triple-Negative Breast Cancer in Syngeneic Mice for Quick and Sequential Progression Analysis of Lung Metastasis. *PLoS ONE* **2018**, *13* (5), e0198143. https://doi.org/10.1371/journal.pone.0198143.

(13) Qu, H.; Fan, C.; Chen, M.; Zhang, X.; Yan, Q.; Wang, Y.; Zhang, S.; Gong, Z.; Shi, L.; Li, X.; Liao, Q.; Xiang, B.; Zhou, M.; Guo, C.; Li, G.; Zeng, Z.; Wu, X.; Xiong, W. Recent Advances of Fluorescent Biosensors Based on Cyclic Signal Amplification Technology in Biomedical Detection. *J Nanobiotechnol* **2021**, *19* (1), 403. https://doi.org/10.1186/s12951-021-01149-z.

(14) Radunz, S.; Tschiche, H. R.; Moldenhauer, D.; Resch-Genger, U. Broad Range ON/OFF PH Sensors Based on PKa Tunable Fluorescent BODIPYs. *Sensors and Actuators B: Chemical* **2017**, *251*, 490–494. https://doi.org/10.1016/j.snb.2017.05.080.

(15) Marshall, J.; Johnsen, S. Fluorescence as a Means of Colour Signal Enhancement. *Phil. Trans. R. Soc. B* **2017**, *372* (1724), 20160335. https://doi.org/10.1098/rstb.2016.0335.

(16) Piston, D. W. *Education in Microscopy and Digital Imaging*. https://zeiss-campus.magnet.fsu.edu/articles/probes/fpintroduction.html.

(17) Mooney, A. M. *Jablonski Diagram of Fluorescence*.

(18) Lalonde, J. M.; Bernlohr, D. A.; Banaszak, L. J. The Up-and-down B-barrel Proteins. *FASEB j.* **1994**, *8* (15), 1240–1247. https://doi.org/10.1096/fasebj.8.15.8001736.

(19) Close, D. W.; Paul, C. D.; Langan, P. S.; Wilce, M. C. J.; Traore, D. A. K.; Halfmann, R.; Rocha, R. C.; Waldo, G. S.; Payne, R. J.; Rucker, J. B.; Prescott, M.; Bradbury, A. R. M. Thermal Green Protein, an Extremely Stable, Nonaggregating Fluorescent Protein Created by Structure-Guided Surface Engineering: Extremely Stable FP Structures and Engineering. *Proteins* **2015**, *83* (7), 1225–1237. https://doi.org/10.1002/prot.24699.

(20) Naveed, H.; Liang, J. Weakly Stable Regions and Protein-Protein Interactions in Beta-Barrel Membrane Proteins. *CPD* **2014**, *20* (8), 1268–1273. https://doi.org/10.2174/13816128113199990071.

(21) Dai, M.; Fisher, H. E.; Temirov, J.; Kiss, C.; Phipps, M. E.; Pavlik, P.; Werner, J. H.; Bradbury, A. R. M. The Creation of a Novel Fluorescent Protein by Guided Consensus Engineering. *Protein Engineering, Design and Selection* **2007**, *20* (2), 69–79. https://doi.org/10.1093/protein/gzl056.

(22) Kiss, C.; Temirov, J.; Chasteen, L.; Waldo, G. S.; Bradbury, A. R. M. Directed Evolution of an Extremely Stable Fluorescent Protein. *Protein Engineering Design and Selection* **2009**, *22* (5), 313–323. https://doi.org/10.1093/protein/gzp006.

(23) Ebisawa, T.; Yamamura, A.; Kameda, Y.; Hayakawa, K.; Nagata, K.; Tanokura, M. The Structure of MAG, a Monomeric Mutant of the Green Fluorescent Protein Azami-Green, Reveals the Structural Basis of Its Stable Green Emission. *Acta Crystallogr F Struct Biol Cryst Commun* **2010**, *66* (5), 485–489. https://doi.org/10.1107/S1744309110011127.

(24) Anderson, M. R.; Padgett, C. M.; Dargatz, C. J.; Nichols, C. R.; Vittalam, K. R.; DeVore, N. M. Engineering a Yellow Thermostable Fluorescent Protein by Rational Design. *ACS Omega* **2023**, *8* (1), 436–443. https://doi.org/10.1021/acsomega.2c05005.

(25) Shaner, N. C.; Campbell, R. E.; Steinbach, P. A.; Giepmans, B. N. G.; Palmer, A. E.; Tsien, R. Y. Improved Monomeric Red, Orange and Yellow Fluorescent Proteins Derived from Discosoma Sp. Red Fluorescent Protein. *Nat Biotechnol* **2004**, *22* (12), 1567–1572. https://doi.org/10.1038/nbt1037.

(26) Don Paul, C.; Traore, D. A. K.; Byres, E.; Rossjohn, J.; Devenish, R. J.; Kiss, C.; Bradbury, A.; Wilce, M. C. J.; Prescott, M. Expression, Purification, Crystallization and Preliminary X-Ray Analysis of ECGP123, an Extremely Stable Monomeric Green Fluorescent Protein with Reversible Photoswitching Properties. *Acta Crystallogr F Struct Biol Cryst Commun* **2011**, *67* (10), 1266–1268. https://doi.org/10.1107/S1744309111028156.

(27) Cai, H.; Yao, H.; Li, T.; Hutter, C. A. J.; Li, Y.; Tang, Y.; Seeger, M. A.; Li, D. An Improved Fluorescent Tag and Its Nanobodies for Membrane Protein Expression, Stability Assay, and Purification. *Commun Biol* **2020**, *3* (1), 753. https://doi.org/10.1038/s42003-020-01478-z.

(28) Velappan, N.; Close, D.; Hung, L.-W.; Naranjo, L.; Hemez, C.; DeVore, N.; McCullough, D. K.; Lillo, A. M.; Waldo, G. S.; Bradbury, A. R. M. Construction, Characterization and Crystal Structure of a Fluorescent Single-Chain Fv Chimera. *Protein Engineering, Design and Selection* **2021**, *34*, gzaa029. https://doi.org/10.1093/protein/gzaa029.

(29) McKinnon, K. M. Flow Cytometry: An Overview. *CP in Immunology* **2018**, *120* (1). https://doi.org/10.1002/cpim.40.

(30) Shaner, N. C.; Patterson, G. H.; Davidson, M. W. Advances in Fluorescent Protein Technology. *Journal of Cell Science* **2007**, *120* (24), 4247–4260. https://doi.org/10.1242/jcs.005801.

(31) Nagai, T.; Ibata, K.; Park, E. S.; Kubota, M.; Mikoshiba, K.; Miyawaki, A. A Variant of Yellow Fluorescent Protein with Fast and Efficient Maturation for Cell-Biological Applications. *Nat Biotechnol* **2002**, *20* (1), 87–90. https://doi.org/10.1038/nbt0102-87.

(32) Griesbeck, O.; Baird, G. S.; Campbell, R. E.; Zacharias, D. A.; Tsien, R. Y. Reducing the Environmental Sensitivity of Yellow Fluorescent Protein. *Journal of Biological Chemistry* **2001**, *276* (31), 29188–29194. https://doi.org/10.1074/jbc.M102815200.

(33) Sabban, S. Development of an in Vitro Model System for Studying the Interaction of Equus Caballus LgE with Its High-Affinity Fc Receptor, The University of Sheffield. https://etheses.whiterose.ac.uk/2040/2/Sabban,_Sari.pdf.

(34) *Visible and Ultraviolet Spectroscopy*. https://www2.chemistry.msu.edu/faculty/reusch/virttxtjml/spectrpy/uv-vis/spectrum.htm.

(35) Khrameeva, E. E.; Drutsa, V. L.; Vrzheshch, E. P.; Dmitrienko, D. V.; Vrzheshch, P. V. Mutants of Monomeric Red Fluorescent Protein MRFP1 at Residue 66: Structure Modeling by Molecular Dynamics and Search for Correlations with Spectral Properties. *Biochemistry Moscow* **2008**, *73* (10), 1085–1095. https://doi.org/10.1134/S0006297908100040.

(36) Wachter, R. M.; Elsliger, M.-A.; Kallio, K.; Hanson, G. T.; Remington, S. J. Structural Basis of Spectral Shifts in the Yellow-Emission Variants of Green Fluorescent Protein. *Structure* **1998**, *6* (10), 1267–1277. https://doi.org/10.1016/S0969-2126(98)00127-0.

(37) Liu, Y.; Ke, M.; Gong, H. Protonation of Glu 135 Facilitates the Outward-to-Inward Structural Transition of Fucose Transporter. *Biophysical Journal* **2015**, *109* (3), 542–551. https://doi.org/10.1016/j.bpj.2015.06.037.